Molecular Signature Associated With Acute Rejection in Vascularized Composite Allotransplantation

Michael F. Cassidy, MD,[1] Nicole A. Doudican, PhD,[2] Nicholas Frazzette, MD,[2] Piul S. Rabbani, PhD,[1] John A. Carucci, MD, PhD,[2] Bruce E. Gelb, MD,[3] Eduardo D. Rodriguez, MD, DDS,[1] Catherine P. Lu, PhD,[1] and Daniel J. Ceradini, MD[1]

Background. A deeper understanding of acute rejection in vascularized composite allotransplantation is paramount for expanding its utility and longevity. There remains a need to develop more precise and accurate tools for diagnosis and prognosis of these allografts, as well as alternatives to traditional immunosuppressive regimens. **Methods.** Twenty-seven skin biopsies collected from 3 vascularized composite allotransplantation recipients, consisting of face and hand transplants, were evaluated by histology, immunohistochemistry staining, and gene expression profiling. **Results.** Biopsies with clinical signs and symptoms of rejection, irrespective of histopathological grading, were significantly enriched for genes contributing to the adaptive immune response, innate immune response, and lymphocyte activation. Inflammation episodes exhibited significant fold change correlations between the face and hands, as well as across patients. Immune checkpoint genes were upregulated during periods of inflammation that necessitated treatment. A gene signature consisting of *CCL5*, *CD8A*, *KLRK1*, and *IFNγ* significantly predicted inflammation specific to vascularized composite allografts that required therapeutic intervention. **Conclusions.** The mechanism of vascularized composite allograft-specific inflammation and rejection appears to be conserved across different patients and skin on different anatomical sites. A concise gene signature can be utilized to ascertain graft status along with a continuous scale, providing valuable diagnostic and prognostic information to supplement current gold standards of graft evaluation.

(*Transplantation Direct* 2024;10: e1714; doi: 10.1097/TXD.0000000000001714.)

Received 6 August 2024. Revision received 12 August 2024.

Accepted 13 August 2024.

[1] Hansjörg Wyss Department of Plastic Surgery, NYU Langone Health, New York, NY.

[2] Ronald O. Perelman Department of Dermatology, NYU Langone Health, New York, NY.

[3] Transplant Institute, NYU Langone Health, New York, NY.

Supported by the Department of Defense Reconstructive Transplantation Research Award (W81XWH-15-2-0036).

The authors declare no conflicts of interest.

M.F.C., E.D.R., C.P.L., and D.J.C. were involved in research design and conceptualization. M.F.C., N.A.D., and N.F. conducted experiments. N.A.D., P.S.R., J.A.C., and C.P.L. provided laboratory resources and oversaw experiments. M.F.C. and N.F. were involved in data analysis. M.F.C., B.E.G., C.P.L., and D.J.C. wrote the article.

Supplemental digital content (SDC) is available for this article. Direct URL citations appear in the printed text, and links to the digital files are provided in the HTML text of this article on the journal's Web site (www.transplantationdirect.com).

Correspondence: Daniel J. Ceradini, MD, Hansjörg Wyss Department of Plastic Surgery, NYU Langone Health, 222 E 41st St, New York, NY 10017. (daniel.ceradini@nyulangone.org); Catherine P. Lu, PhD, Hansjörg Wyss Department of Plastic Surgery, NYU Langone Health, 222 E 41st St, New York, NY 10017 (pei-ju.lu@nyulangone.org).

ISSN: 2373-8731

DOI: 10.1097/TXD.0000000000001714

Vascularized composite allotransplantation (VCA), defined as the transplantation of multiple tissue types such as the skin, muscle, nerve, and bone as a functional unit, is indicated for patients with devastating soft tissue injuries that are not ameliorable to autologous reconstruction alone. Despite substantial surgical advances, acute rejection (AR) remains a significant obstacle. Approximately 85% of patients will experience a rejection episode within the first postoperative year,[1] thereby limiting its widespread use as a restorative treatment option.

The current gold standard for grading VCA rejection is defined by the 2007 Banff working classification, which evaluates perivascular and epidermal infiltration.[2] Although credited with providing a systematic framework for describing histological findings, its limitations include intra- and interobserver variability, particularly when distinguishing grade I and grade II rejection.[3] Similarly, recent studies suggest that grade I rejection does not represent a pathological state, demonstrated by a lack of differential expression at the RNA level.[4] Furthermore, no correlation has been established between Banff grade and the need for treatment.[3,5]

Complicating this are inflammatory skin conditions masquerading as rejection, mimicking both histological and clinical findings.[5,6] A deeper understanding of the molecular mechanisms of VCA rejection is necessary to resolve these conflicts in diagnosis and treatment. Although current corollaries are derived from principles in solid organ transplantation (SOT), VCA uniquely incorporates the skin, a highly

immunogenic organ. Aside from its barrier function, the skin contains appendages that secrete antimicrobial molecules, Langerhans cells that sample and present antigens, and tissue-resident leukocytes that mediate effector functions, collectively orchestrating a complex immune response.[7,8] At the foundational level, possible variation across patients or recipient anatomical sites of transplantation has not been fully investigated. Although there are some data suggesting disparate histopathological findings between oral mucosa and skin in VCA,[9,10] it is unknown whether differences in skin infiltration exist between face and hand transplants.

Herein, we investigate the transcriptomic landscape of VCA rejection in human face and hand specimens from three different patients, yielding a list of differentially expressed genes (DEGs) and enrichment for key molecular pathways. Applying the same approach, we then survey samples with discordant histological and clinical findings to better understand their underlying diagnoses. Finally, we compare our results to an external dataset to develop and validate a concise gene signature for VCA graft monitoring.

MATERIALS AND METHODS

Sample Collection

Skin punch biopsies were longitudinally collected from 3 patients with VCA. All patients underwent face transplantation, with patient 1 concomitantly undergoing bilateral hand transplantations. RNA was isolated from a total of 27 formalin-fixed, paraffin-embedded (FFPE) biopsies using the Qiagen RNeasy FFPE kit according to product guidelines. All specimens passed quality control parameters (RNA concentration > 100μg, A260/A280 ratio > 1.5) and underwent gene expression profiling using the NanoString nCounter Human Organ Transplant Panel.

Sample Status

Sample status was determined using a holistic approach, incorporating Banff grade, clinical appearance, and subjective patient experience. Final diagnoses were agreed upon after discussions between clinicians in plastic surgery, transplant surgery/immunology, and dermatopathology. This clinicopathologic correlation is imperative in determining diagnoses and treatment approaches in VCA recipients.[3] The 27 biopsy specimens were initially categorized as the following: nonrejection (NR, n = 6), AR (n = 9), and inflammatory reaction (IR, n = 12; Table 1). NR was defined as *concordant* clinical and histological findings (Banff grade ≤ I; **Figure S1, SDC,** http://links.lww.com/TXD/A702) that did not suggest rejection. AR was defined as *concordant* clinical and histological findings (Banff grade ≥ II; **Figures S2 and S3, SDC,** http://links.lww.com/TXD/A702), indicating active rejection and necessitating inpatient immunosuppression. IR was defined as *discordant* clinical and histological findings; specifically, the patient exhibited clinical findings consistent with rejection (eg, erythema, edema,

TABLE 1.

Summary of sample collection and status

				Banff grade				
Sample #	POD	Site	Patient	Infiltrate	Interface	Final dermatopathology Status	Clinical status	Final holistic status
1	27	Face	1	1	0	NR	NR	NR
2	43	Face	1	1	0	NR	NR	NR
3	83	Face	1	1	0	NR	NR	NR
4	280	Face	1	2	3	AR	AR	AR
5	280	Hand	1	2	3	AR	AR	AR
6	280	Hand	1	2	3	AR	AR	AR
7	280	Hand	1	2	3	AR	AR	AR
8	392	Hand	1	2	3	AR	AR	AR
9	392	Hand	1	2	3	AR	AR	AR
10	392	Face	1	1	3	NR	AR	IR
11	426	Face	1	1	3	NR	AR	IR
12	426	Hand	1	1	3	NR	AR	IR
13	462	Face	1	1	3	NR	AR	IR
14	462	Hand	1	1	3	NR	AR	IR
15	539	Face	1	1	3	NR	NR	NR
16	610	Face	1	1	3	NR	AR	IR
17	698	Face	1	1	3	NR	AR	IR
18	698	Hand	1	1	3	NR	AR	IR
19	698	Hand	1	1	3	NR	AR	IR
20	749	Face	1	1	3	NR	AR	IR
21	749	Hand	1	1	3	NR	AR	IR
22	749	Hand	1	1	3	NR	AR	IR
23	47	Face	2	1	3	NR	NR	NR
24	537	Face	2	1	2	AR	AR	AR
25	586	Face	2	1	3	AR	AR	AR
26	1291	Face	3	1	2	NR	NR	NR
27	1465	Face	3	2	3	AR	AR	AR

Corresponding patient, biopsy site, Banff grade (including breakdown of inflammatory infiltrate and interface changes), clinical status, and final holistic status of each biopsy specimen.
AR, acute rejection; IR, inflammatory reaction; NR, nonrejection; POD, postoperative day.

desquamative rash, pain) without supporting histological findings (Banff Grade ≤ I; **Figure S4, SDC,** http://links.lww.com/TXD/A702). These samples resulted in therapeutic intervention as well.

Clinical Maintenance, Evaluation, and Treatment of AR

All patients with VCA at our institution received T and B cell–depleting induction therapy with thymoglobulin and rituximab, respectively. Three-drug maintenance immunosuppression consisted of tacrolimus, prednisone, and mycophenolate mofetil. Therapeutic interventions for AR commonly included a pulse steroid taper, in addition to possible adjuncts such as tacrolimus dose adjustment, plasmapheresis, and antihistamines depending on the presumed cause. After resolution of rejection, all patients were re-evaluated shortly thereafter in the clinic. Tacrolimus trough levels were monitored and adjusted as needed.

Statistical Analysis

A full description of the statistical methods can be found in the **Supplemental Digital Content** (http://links.lww.com/TXD/A702). Briefly, raw RNA transcript counts were analyzed according to the NanoTube package guidelines.[11] DEG criteria included P_{adj} <0.05 and $|\log_2 FC| \geq 1$. An elastic net regression was utilized to create a gene signature (hereafter referred to as "Inflammation Score") diagnostic of biopsies with significant inflammation, which was subsequently validated using data from Win et al.[4]

Study Approval

Protocols of this study were conducted with IRB approval (Protocol i14-00550) in accordance with Code of Federal Regulations on the Protection of Human Subjects (45 CFR Part 46) and adhere to the ethical principles based on Good Clinical Practice, Declaration of Helsinki, and ICH Guidelines. Written informed consent was provided for the use of patient photographs and the record of informed consent was retained. All photograph copyrights are retained by Eduardo D. Rodriguez, MD, DDS.

RESULTS

AR and IR Biopsies Share DEGs

Routine NR monitoring visits displayed graft skin color akin to surrounding native tissue, devoid of significant edema, cutaneous lesions, or eruptions (Figure 1A). Episodes of AR manifested clinically with graft erythema, edema, and pain (Figure 1B). The average time from transplant to first rejection episode was 511 d (range 280–715; data not shown). Upon principal component analysis of the gene expression data, AR samples expectedly clustered together, separately from NR samples (Figure 1C). Interestingly, IR samples clustered very closely with AR, suggesting similarities in gene expression. To further explore these observations, a heatmap with unsupervised hierarchical clustering of genes and samples was created. To parse out several possible patterns, samples were annotated by biopsy site, patient of origin, and holistic status. Seven of 9 AR samples clustered separately from NR samples again (Figure 1D). Similar to our principal component analysis results, IR samples were interspersed within AR samples. We did not observe any secondary pattern such as clustering by patient or anatomical site, as these characteristics were heterogeneously distributed.

Differential expression analysis was performed to ascertain DEGs in AR and IR compared with NR, inclusive of all patients and anatomical sites. AR samples yielded 140 DEGs, with the most upregulated by t-statistic being the T-cell chemokine *CCL5* (*RANTES*), T-cell coreceptor *CD8A*, interferon-inducible inflammasome molecule *AIM2*, proapoptotic molecule *FASLG*, and checkpoint receptor *LAG3* (Figure 1E; **Table S1, SDC,** http://links.lww.com/TXD/A702). Immunohistochemistry staining for *CD8* confirmed its upregulation in AR biopsies (**Figures S2C and S3C, SDC,** http://links.lww.com/TXD/A702). IR samples yielded 165 DEGs, the most upregulated being the T-cell chemokine *XCL1/2*, transcriptional regulator *STAT1*, immunoglobulin receptor *FCGR1A*, *CCL5*, and *CD8A* (Figure 1F; **Table S2, SDC,** http://links.lww.com/TXD/A702). AR and IR specimens shared 108 DEGs, which were very highly correlated according to t-statistic (Pearson $r = 0.95$, $P < 0.001$) and $\log_2 FC$ (Pearson $r = 0.95$, $P < 0.001$). Four genes were significantly upregulated (*PTX3*, *COL4A4*, *THBS1*, and *TNFRSF18*), and 1 gene was significantly downregulated (*CLEC4C*) in IR samples compared with AR. Aggregating AR and IR specimens yielded 152 DEGs compared with NR, which were enriched for pathways related to the adaptive and innate immune responses, cytokine signaling, and T /natural killer cell–mediated cytotoxicity (Figure 1G).

Inflammatory Mechanisms Are Conserved Across Anatomical Sites

Given the striking similarities in gene expression between episodes of definitive AR and IRs, these samples were aggregated for all subsequent analyses to investigate graft inflammation irrespective of the original cause (hereafter referred to as "inflamed" samples). Potential differences across anatomical sites, namely the face and hands, were assessed first. We controlled for different patients by analyzing only inflamed samples from patient 1. Heatmap clustering of AR and IR samples from the face and hands revealed largely conserved patterns across biopsy sites (Figure 2A). Across the entire NanoString panel, we observed significant correlations in gene fold changes agnostic of the site of inflammation (all Pearson $r \geq 0.41$, all $P < 0.001$; Figure 2B). Differential gene expression was then performed, comparing (1) inflamed face versus NR and (2) inflamed hands versus NR, *exclusively* in patient 1. Inflamed face samples exhibited 149 DEGs (Figure 2C; **Table S3, SDC,** http://links.lww.com/TXD/A702), whereas inflamed hand specimens exhibited 161 DEGs (Figure 2D; **Table S4, SDC,** http://links.lww.com/TXD/A702). There were no DEGs when comparing inflamed face and inflamed hands directly (Figure 2E). Of the aforementioned 149 and 161 DEGs, 127 DEGs were mutually enriched in both inflamed face and hand specimens (Figure 2F) and demonstrated even stronger fold change correlations (all Pearson $r \geq 0.71$, all $P < 0.001$; data not shown).

Inflammatory Mechanisms Are Conserved Across Patients With VCA

Next, we investigated potential variations in VCA rejection across patients while controlling for anatomical site by only

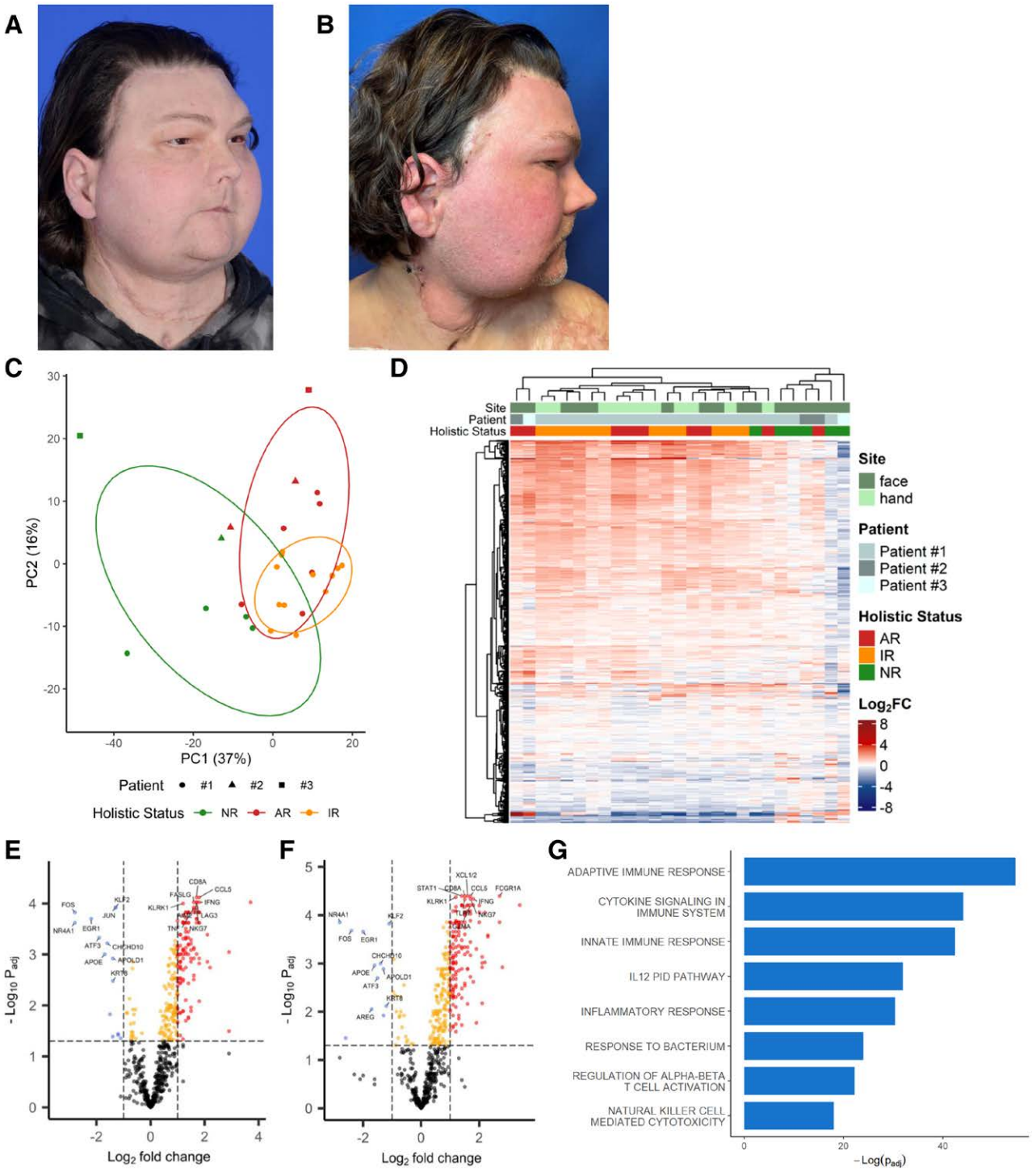

FIGURE 1. Acute rejection and inflammatory reaction biopsies share DEGs. Clinical images demonstrating (A) NR and (B) AR. Clustering by (C) PCA and (D) unsupervised hierarchical heatmap clustering demonstrating colocalization of inflamed biopsies separate from NR. Volcano plots annotated with top DEGs comparing (E) AR to NR and (F) IR to NR. G, Pathway enrichment of DEGs from aggregated AR/IR samples. Printed with permission and copyrights retained by Eduardo D. Rodriguez, MD, DDS. AR, acute rejection; DEG, differentially expressed gene; IL, interleukin; IR, inflammatory reaction; NR, nonrejection; PCA, principal component analysis.

analyzing face specimens. No clear patterns were observed on heatmap clustering (Figure 3A). However, we noted a band of genes that appeared dysregulated between patient 1 and 2/3. These genes coded for immunoglobulin chains, consisting of *IGHG1*, *IGHG2*, *IGHG3*, *IGHG4*, *IGKC*, *IGLC1*, and *IGHA1*. Once again, all samples demonstrated significant fold change correlations with each other, regardless of the patient of origin (all Pearson $r \geq 0.13$, all $P < 0.005$; Figure 3B). Subsequently, differential gene expression analysis compared (1) Patient #1 face inflamed samples versus all NR and (2)

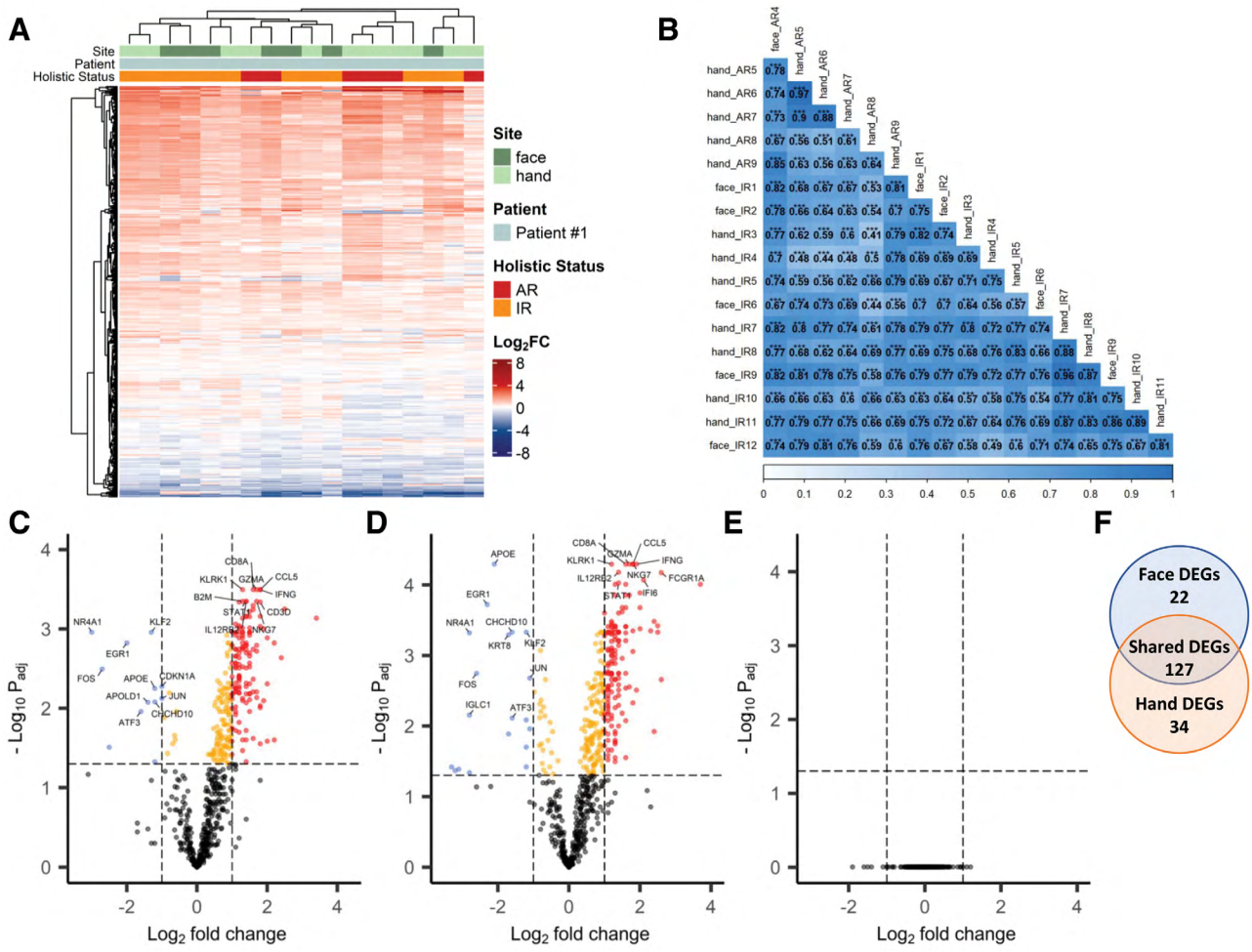

FIGURE 2. Inflammatory mechanisms are conserved across anatomical sites. A, Unsupervised hierarchical heatmap clustering depicting fold changes of inflamed biopsies compared with NR in patient 1. B, Pearson correlation coefficients comparing NanoString panel fold changes between inflamed samples in patient 1. Volcano plots comparing (C) face inflamed vs NR, (D) hand inflamed vs NR, and (E) face vs hand inflamed exclusively in patient 1. F, Venn diagram of mutually enriched DEGs. DEG, differentially expressed gene; NR, nonrejection.

combined patients 2/3 face inflamed versus all NR (NR samples were inclusive of all patients). Inflamed face samples from patient #1 exhibited 151 DEGs (Figure 3C; **Table S5, SDC,** http://links.lww.com/TXD/A702), whereas inflamed samples from patients 2/3 exhibited 127 DEGs (Figure 3D; **Table S6, SDC,** http://links.lww.com/TXD/A702). Interestingly, we discovered that the above-mentioned immunoglobulin genes were significantly upregulated in patients 2/3 compared with patient 1 during episodes of inflammation (Figure 3E; **Table S7, SDC,** http://links.lww.com/TXD/A702). Despite this, 82 DEGs were shared between all patients (Figure 3F) and demonstrated positive fold change correlations (all Pearson $r \geq 0.20$; data not shown).

Immune Checkpoint Genes Are Upregulated During Inflammation

Given the prominent role of T cells in VCA inflammation, immune checkpoint molecules are of interest to attenuate this adaptive immune response. Of the 7 checkpoint genes we investigated, *LAG3*, *CTLA4*, *TIGIT*, *BTLA*, and *CD273* (*PDCD1LG2*) were significantly upregulated in AR and IR biopsies (Figure 4A). Despite the upregulation of its relative *CD273*, *CD274* (*PDCD1LG1*) was not significantly enriched in VCA inflammation.

Concise Inflammation Score Accurately Ascertains Graft Status

Our final aim was to identify key genes implicated in acutely worsening graft status that could be leveraged as potential biomarkers. Given our prior results demonstrating the reliable consistency in gene expression across VCA recipients and anatomical sites, we continued to aggregate AR/IR under "inflamed" samples and compared with NR to maximize statistical power and clinical utility. All genes in the NanoString panel were subjected to an elastic net regression with features defined in the Supporting Information section. A 4-gene signature (Inflammation Score) consisting of *CCL5*, *CD8A*, *KLRK1* (*NKG2D*), and *IFNγ* yielded the best fitting model predictive of inflamed samples, with the following equation:

$$\text{Inflammation Score} = -2.75431007 + 0.409140914(\text{CCL5}) + 0.418182973(\text{CD8A}) + 0.696944365(\text{KLRK1}) + 0.288972349(\textit{IFN}\gamma)$$

Units of measurement were normalized and $\log_{10}$-transformed raw RNA transcript counts. An Inflammation Score >1.010952 was determined to be the threshold for classifying episodes of significant inflammation, likely necessitating treatment. All genes in the signature were significantly

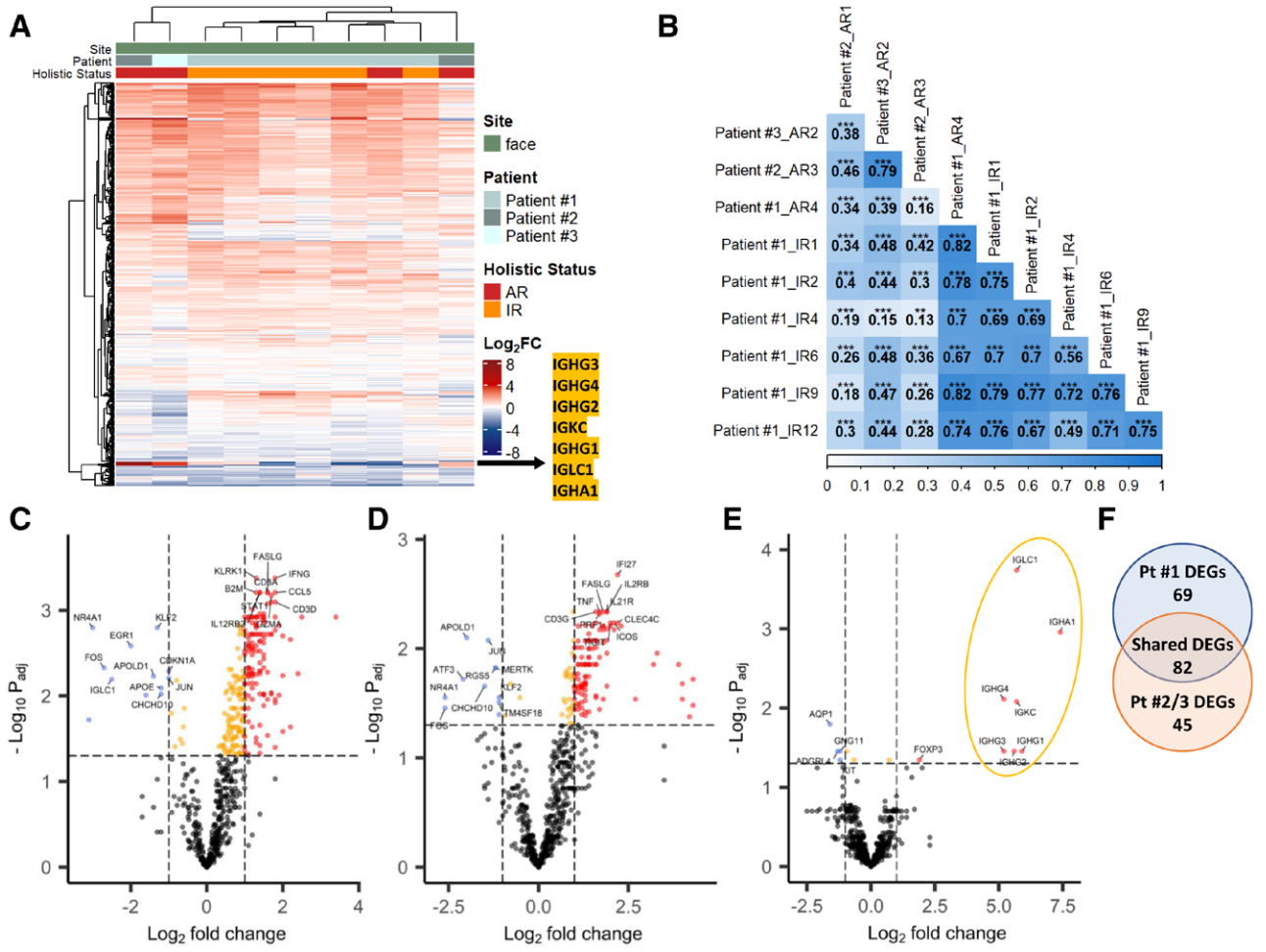

FIGURE 3. Inflammatory mechanisms are conserved across patients with VCA. A, Unsupervised hierarchical heatmap clustering depicting fold changes of face inflamed biopsies compared with NR across patients. B, Pearson correlation coefficients comparing NanoString panel fold changes between face inflamed samples across patients. Volcano plots comparing (C) patient 1 face inflamed vs all NR, (D) patients 2/3 face inflamed vs all NR, and (E) patient 1 vs patients 2/3 face inflamed. F, Venn diagram of mutually enriched DEGs. DEG, differentially expressed gene; NR, nonrejection; VCA, vascularized composite allotransplantation.

upregulated in inflamed biopsies, regardless of the inciting factor (Figure 4B). We then retrospectively and longitudinally plotted the Inflammation Score in biopsies from patient 1, clearly delineating inflamed visits from NR visits (**Figure S5A, SDC,** http://links.lww.com/TXD/A702).

The applicability of this gene signature was determined by validation on an external dataset. Win et al[4] evaluated 35 biopsies from 7 face transplant recipients by NanoString gene expression profiling. Biopsies were graded exclusively by the Banff working classification. *CCL5*, *CD8A*, and *KLRK1* were significantly upregulated in these specimens with grade ≥II inflammation (Figure 4C). Moreover, *CCL5* and *KLRK1* were significantly increased in grades III versus II. Consistent with the authors' results, we did not find any difference in gene expression between grades 0 and I biopsies. Interestingly, *IFNγ* did not significantly correlate with Banff grade in these specimens. Despite this, our Inflammation Score significantly increased in a stepwise manner with Banff grade in this dataset.

Finally, we quantified the diagnostic capacity of our 4-gene signature against both VCA and non-VCA samples from Win et al For this external dataset, we recoded samples into binary classifications as described in the **Supplemental Digital Content** (http://links.lww.com/TXD/A702), such that samples with Banff grade ≥II were considered "inflamed" and all other samples were noninflamed. Our Inflammation Score significantly predicted inflamed biopsies, with an area under the curve = 0.85 (95% confidence interval, 0.71-0.98 by 10 000 bootstrap replicates; Figure 4D). Moreover, we found no significant difference in Inflammation Score between NR and normal skin, delayed-type hypersensitivity reaction (DTH), and rosacea (**Figure S5B, SDC,** http://links.lww.com/TXD/A702).

DISCUSSION

In the present study, we demonstrate that transcriptomic analyses can be used to gain insight into graft status, particularly when there is clinicopathologic discordance and uncertainty. AR and IR likely exhibit similar mechanisms, albeit with different histopathological findings (Figure 1C–G). This is imperative to consider during patient evaluation when reconciling the relative weight of clinical and histological data in forming a diagnostic impression. With respect to the individuality of VCA rejection/inflammation, our analyses consistently demonstrate that these mechanisms are conserved across both anatomical site (Figure 2) and different patients (Figure 3),

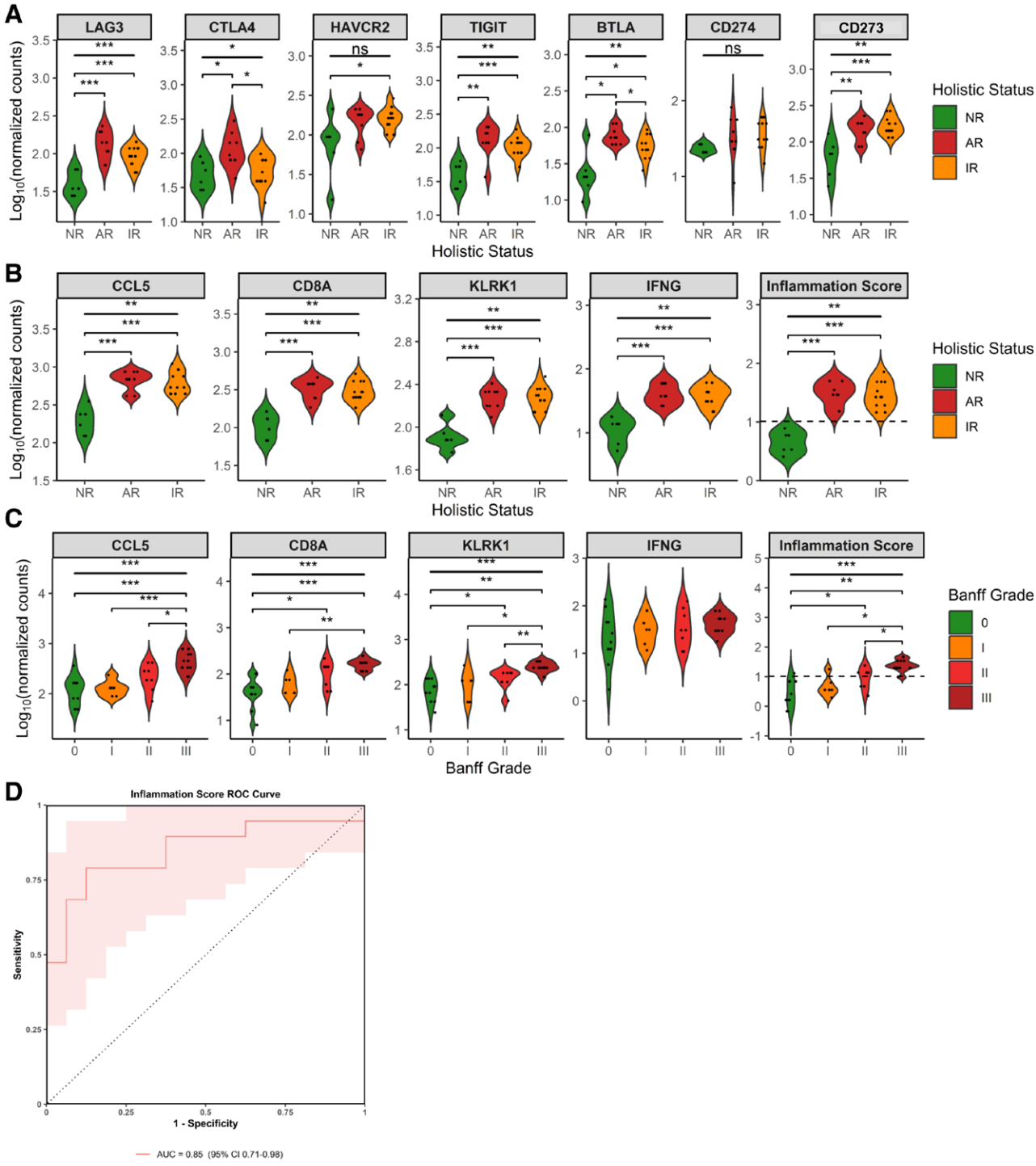

FIGURE 4. Concise Inflammation Score distinguishes graft status. Normalized and log-transformed counts for (A) immune checkpoint genes. Elastic net regression genes with Inflammation Score trained on (B) internal dataset and tested on (C) external dataset. Dotted line represents threshold discriminating significantly inflamed from noninflamed samples. D, ROC curve of Inflammation Score validated on external dataset of VCA and non-VCA biopsies. $^{*}P_{adj} < 0.05$, $^{**}P_{adj} < 0.01$, $^{***}P_{adj} < 0.001$. AR, acute rejection; DEG, differentially expressed gene; IR, inflammatory reaction; NR, nonrejection; ROC, receiver operating characteristic; VCA, vascularized composite allotransplantation.

although with less strength of association across the latter. Finally, we demonstrate that key genes can be integrated into a novel gene signature used for ascertaining graft inflammation which requires clinical intervention (Figure 4B–D).

In the perioperative period, traditional induction therapy has been aimed at T-cell depletion via thymoglobulin and/or anti-*interleukin-2* antibody.[12] The use of B cell–depleting therapy with rituximab is a novel strategy at our institution. B-cell depletion in VCA induction immunosuppression has not been reported, with the exception of the anti-*CD52* antibody alemtuzumab in abdominal wall transplantation, which indiscriminately targets all lymphocytes.[13,14] The benefit of alemtuzumab in SOT is equivocal though, as it may cause B-cell repopulation to levels greater than baseline, increase B

cell–activating factor (*BAFF*), and stimulate de novo donor-specific antibodies (dnDSAs).[15-17] Rituximab, although perhaps not 100% B-cell depleting, markedly reduces the B-cell population, dnDSAs, and biopsy-proven rejection in not only ABO-compatible kidney transplants, but also highly sensitized (panel reactive antibody [PRA] > 50%) transplant recipients.[18-20] Despite the occasional risk of leukopenia, rituximab remains a relatively safe drug with minimal to no additional risk of infection in these cohorts.[21] PRA is an important metric that our VCA team considers when identifying the best possible donor for our patients; in particular, Patient 1 was highly sensitized (PRA > 90%). For these reasons outlined, we believe that rituximab is a critical addition to VCA induction therapy to theoretically mitigate the risk of dnDSAs and their contribution to rejection. It is interesting though that we found significantly elevated levels of immunoglobin chain genes in patients 2/3 compared with patient 1 during graft inflammation (Figure 3A and D). These 2 patients were not highly sensitized, which might suggest that rituximab has a greater benefit in patients with higher sensitization and, therefore, more prone to antibody-mediated rejection. These conclusions remain theoretical and further studies are needed to determine the true benefit of B-cell depletion in patients with different levels of PRA. One of the arguments against B-cell depletion is the reduction in regulatory B-cell populations (Breg). Much like regulatory T cells (Treg), Breg can attenuate the immune response. Although thymoglobulin has been shown to actually induce a Treg phenotype, the same cannot be as clearly stated for B cell–depleting agents.[22] There are data though that suggest B-cell depletion may prolong graft survival when the alloantigen load is low or when T-cell depletion is used in conjunction (as in our induction protocol).[23-25] Therefore, we advocate for the addition of rituximab with thymoglobulin.

Little is known regarding the variation of VCA rejection between skin on the face and hands, particularly because these surfaces interact with objects and at different magnitudes and frequencies. Hands act as the primary physical interface with the external environment, exerting forces to grab, push, and twist objects. Moreover, contributions from the skin microbiome cannot be overlooked; hand microbiota has demonstrated greater diversity and variability than other skin regions, largely influenced by individuals' daily activities.[26-28] Conversely, the face rarely touches objects directly and includes the mucosal surfaces of the mouth, nose, and eyes, contributing their own microenvironments. As a result, there may exist differential risks of infection, microtrauma, and other inciting factors of rejection depending on the allograft site. There is only cursory data from Kanitakis et al, who describe consistently elevated rejection grades in oral mucosa compared with face skin in their face transplant recipient, though not significant due to sample size.[10] The authors attribute this increased inflammation to the antigenicity of the mucosa, distribution of antigen-presenting cells (APCs), and more frequent viral/fungal infections of the oral cavity. Although these results are intriguing, we demonstrate no significant transcriptomic differences in rejection/inflammation between face and hand skin biopsies (Figure 2). Altogether, these results suggest the type of epithelium itself plays a larger role in VCA rejection rather than skin location.

Importantly though, we note the enrichment of pathways related to innate immunity, nonspecific inflammation, and external stimuli/pathogens, suggesting these as potential culprits contributing to rejection and highlighting the importance of the skin's barrier function. DEGs contributing to these pathways include the microbial ssRNA sensors *TLR7*/*TLR8*, antibody-dependent cellular cytotoxicity mediators *FCGR1A*/*FCGR3A*, and physical stimuli sensor *NR4A1*, to name a few. The upregulation of these genes related to environmental antigen sampling and stimuli detection are of interest for the development of topical treatments that exert their effects locally instead of systemically.

As slightly >100 patients worldwide have undergone VCA, its rejection immunopathogenesis has been challenging to compare across patients.[29,30] A strength of our data is the ability to compare these mechanisms across 3 patients, including the first successful combined face and double-hand transplant performed to date.[31] Allograft procurement is an extensive process, assessing factors such as recipient antibody profile, donor demographics and comorbidities, and anatomical structure among others. Given the individuality of candidate selection, the mechanisms of VCA rejection may exhibit equally unique nuances across recipients. Notably, we discovered several immunoglobulin-coding genes to be significantly upregulated in patients 2/3 compared with patient 1 (Figure 3A and E). This was initially puzzling, as all 3 patients received rituximab during induction therapy to theoretically prevent de novo alloantibody formation.[32,33] We speculate that differences in immunoglobulin expression may result from different volumes of vascularized bone marrow (VMB) across patients.[34] However, the effects of B cell–depleting induction therapy and VBM volume on VCA rejection remain to be fully explored.

As immune checkpoint inhibitors have evolved into standard treatment options for certain cancers, the prospect of agonist molecules has gained traction in the fields of autoimmunity and transplantation. Our NanoString panel evaluated 7 immune checkpoint genes, 5 of which were significantly upregulated in inflamed VCA biopsies: *CTLA4*, *TIGIT*, *BTLA*, *PDCD1LG2*, and the most significantly enriched, *LAG3* (Figure 4A). Perhaps, the most clinically utilized checkpoint inhibitor is anti-*PD-1*/*PD-L1*, now indicated for a variety of cancers refractory to traditional therapies. However, more than half of patients have failed to respond to these checkpoint inhibitors because of nuances in their mechanism of action.[35] Our results, in conjunction with recent literature, favor *LAG3* as a promising target. Blockade and deletion of *LAG3* has been shown to increase accumulation and effector function of antigen-specific CD8 T cells within organs and tumors expressing cognate antigens.[36] Agonism of this molecule may exert the opposite effect, thereby reducing intragraft cytotoxicity. Two *LAG3* agonist antibodies, IMP761 and GSK2831781, are currently under investigation. IMP761 has demonstrated a dose-dependent inhibition of CD8 T-cell activation in vitro and reduced T-cell infiltration of DTH sites in nonhuman primates.[37] The mechanism for GSK2831781 is slightly different, inducing antibody-dependent cellular cytotoxicity of target cells after binding, thereby depleting *LAG3*-expressing cells. In a phase I clinical trial for the treatment of psoriasis, GSK2831781 exhibited a dose-dependent depletion of both *LAG3*$^+$ peripheral blood mononuclear cells and *LAG3*$^+$ intralesional T cells, reduction in proinflammatory genes, and clinical improvement.[38] *LAG3* is also a unique target for its role in plasma cells. A recent study uncovered a population of *LAG3*$^+$ regulatory plasma cells, which rapidly produces interleukin-10 after toll-like receptor stimulation.[39]

These data support our proposition of *LAG3* as a potential immunoregulatory target and an important link between T cells and B cells.

Our study advances clinical diagnosis in VCA through the development of an objective molecular signature for ascertaining graft status. Genes contributing to this Inflammation Score included *CCL5*, *CD8A*, *KLRK1*, and *IFNγ* (Figure 4B), all of which except *IFNγ* have previously demonstrated increased expression in rejection biopsies from human face transplants.[4]

The T-cell chemokine *CCL5* contributes to graft dysfunction and loss in SOT.[40] Intriguingly, *CCL5* expression has also exhibited a stepwise increase in an animal model of normal skin, syngeneic, and allogeneic vascularized groin transplants, respectively.[41] This illustrates *CCL5*'s differential role in mediating both innate and adaptive immunity, which can be leveraged to potentially distinguish different sources of graft inflammation. It is well-established that *CD8A* plays a role in T cell–mediated rejection in SOT, as alloreactive cytotoxic T cells mediate graft damage via granzymes and perforins.[42] Similarly, *KLRK1* is an activating receptor on the surface of NK and T cells, providing costimulation in a manner akin to *CD28*.[43] Ligands of *KLRK1* are major histocompatibility complex class I chain-related antigens A and B (*MICA*/*MICB*), which are expressed on endothelial cells, keratinocytes, and monocytes.[44] Blockade of *KLRK1* has been shown to prolong allograft survival in murine cardiac and bone marrow transplant models.[43] Additionally, the upregulation of *MICA*/*MICB* are specific to *allograft* rejection in a skin transplant model, as this change has not been observed in healing syngeneic skin transplants in the same recipient animals.[45] Aside from its costimulatory function, the soluble form of *KLRK1* ligands surprisingly produces the opposite effect. The soluble form of *MICA* correlates with good graft status in cardiac transplants because this form induces endocytosis and degradation of *KLRK1* upon binding.[43] Overall, blockade of *KLRK1* and exogenous, soluble forms of its ligands may represent unique strategies in VCA immunotherapy. Finally, *IFNγ* represents a universal transcript of transplant rejection, orchestrating numerous molecular programs such as *IFNγ*-inducible changes to the endothelium, effector functions, and chemokine production.[46] Consistent with these effects is the enrichment of the *IL12* pathway, an upstream regulator of *IFNγ* expression, in our inflamed biopsies (Figure 1G). It is intriguing that the study by Win et al did not find a significant increase in *IFNγ*. A prior study by this group (analyzing 6 of their 7 face transplant patients) demonstrated a significant increase in intragraft *IFNγ*-producing T cells and peripheral blood *IFNγ*-producing CD8 T cells during rejection when compared with pre- and postrejection timepoints.[47]

It is important to recognize why we chose to combine AR and IR biopsies for training the Inflammation Score model. First, our early results demonstrated very few transcriptomic differences between these original categories (Figure 1C–F). Second, every AR and IR episode warranted clinical intervention, commonly pulse steroids, irrespective of the inciting cause (definitive rejection versus inflammation secondary to another cause). Therefore, we determined it to be more clinically useful to create a gene signature based on the need for treatment. To the best of our knowledge, this is the first time a single metric has been created to significantly predict the need for treatment in VCA rejection.

In a similar vein, it is important to clarify the histologic discrepancies during IR episodes. Every IR biopsy was classified as grade I inflammatory infiltrate (mild perivascular) and grade III interface change (apoptosis, dyskeratosis, and/or keratinolysis). The reason why these biopsies were not classified overall as grade III rejection was because there was usually only one or two apoptotic keratinocytes present. These cells were quite rare, did not appear to reflect the entire specimen, and we believe these might not even be detected by all dermatopathologists. Nevertheless, even the existence of a single apoptotic cell technically renders a classification of grade III rejection. This dilemma has been encountered by other groups in the field of VCA, expressing similar uncertainty regarding treatment.[10]

Altogether, our Inflammation Score is not intended to replace clinicopathologic evaluation of composite tissue allografts, but rather be used as an adjunct diagnostic tool to this gold standard. Indeed, we have outlined challenges with the Banff grading system, and discordance between histological and clinical findings exists. Our gene signature offers diagnostic clarity when uncertainty arises, including distinguishing non-VCA inflammatory skin conditions. Although some genes were differentially expressed when comparing NR to normal skin, DTH, and rosacea, the Inflammation Score as a whole showed no significant difference among these diagnoses, suggesting our model is greater than the sum of its parts. This is critical in ruling out rejection and avoiding unnecessary pulse steroids. Importantly, obtaining these results requires no additional tissue harvesting, since biopsies are already performed for evaluation by our dermatopathology team; NanoString utilizes tissue sections from these same FFPE blocks. However, less invasive diagnostic tools are still needed, such as epidermal stripping, as any biopsy may produce an inflammatory response of its own.[48] Another application of our Inflammation Score is longitudinal graft monitoring on a continuous scale, compared with the ordinal scale of Banff. This allows clinicians to trend graft status as it approaches the threshold denoting significant inflammation and preemptively titrate immunosuppression to curb impending rejection. This is imperative because of the additive effect of repeated AR episodes on chronic allograft dysfunction in both human SOT and animal VCA models.[49]

Limitations of our study pertain mostly to sample size. There were relatively few biopsies from patients 2/3, requiring their pooling for analyses. Consequently, this limits the external validity of our gene signature, which should be cautioned against overinterpretation. Similarly, we did not acquire any NR specimens from the hands, precluding an accurate baseline assessment for this site. The relative infrequency of rejection episodes was also a challenge for sample collection, as the average time from transplant to first AR was 511 d, possibly because of the protective effect of VBM or B cell–depleting induction therapy. Regarding the external dataset used, we were unable to directly compare results due to the use of different NanoString panels with only ~50% overlap in genes. Despite this, it is reassuring that genes contributing to our Inflammation Score were validated. Moreover, the NanoString panel is a curated list of genes that are most likely to be enriched in transplant pathologies. We recognize that gene profiling using this panel is almost self-fulfilling, and the use of unrestricted RNA sequencing techniques may identify additional enriched genes.

In this study, we interrogated skin biopsies from three VCA recipients using NanoString gene expression profiling. Exploring the diagnoses of NR, AR, and clinicopathological discordance (IR), we concluded that inflammatory and rejection mechanisms in VCA are relatively conserved across the face and hands, as well as between patients. Supporting prior literature, immune checkpoint molecules were significantly upregulated during episodes of graft inflammation. Finally, we developed a concise gene signature that is associated with significant graft inflammation and augments the clinicopathologic evaluation of VCA rejection. Altogether, we contribute to the foundation of translational VCA research for the development of novel biomarkers and therapeutics.

ACKNOWLEDGMENTS

We would like to express our utmost gratitude to the patients in this study for their participation and continued support. We also thank Dr. Shane Meehan for providing expertise in dermatopathology and microscopy images.

REFERENCES

1. Petruzzo P, Lanzetta M, Dubernard JM, et al. The international registry on hand and composite tissue transplantation. *Transplantation*. 2010;90:1590–1594.
2. Cendales LC, Kanitakis J, Schneeberger S, et al. The Banff 2007 working classification of skin-containing composite tissue allograft pathology. *Am J Transplant*. 2008;8:1396–1400.
3. Schneider M, Cardones ARG, Selim MA, et al. Vascularized composite allotransplantation: a closer look at the Banff working classification. *Transpl Int*. 2016;29:663–671.
4. Win TS, Crisler WJ, Dyring-Andersen B, et al. Immunoregulatory and lipid presentation pathways are upregulated in human face transplant rejection. *J Clin Invest*. 5166;131:e13.
5. Sarhane KA, Khalifian S, Ibrahim Z, et al. Diagnosing skin rejection in vascularized composite allotransplantation: advances and challenges. *Clin Transplant*. 2014;28:277–285.
6. Colamatteo A, Carbone F, Bruzzaniti S, et al. Molecular mechanisms controlling foxp3 expression in health and autoimmunity: from epigenetic to post-translational regulation. *Front Immunol*. 2020;10:3136.
7. Kabashima K, Honda T, Ginhoux F, et al. The immunological anatomy of the skin. *Nat Rev Immunol*. 2019;19:19–30.
8. Nguyen AV, Soulika AM. The dynamics of the skin's immune system. *Int J Mol Sci*. 2019;20:1811.
9. Bergfeld W, Klimczak A, Stratton JS, et al. A four-year pathology review of the near total face transplant. *Am J Transplant*. 2013;13:2750–2764.
10. Kanitakis J, Badet L, Petruzzo P, et al. Clinicopathologic monitoring of the skin and oral mucosa of the first human face allograft: report on the first eight months. *Transplantation*. 2006;82:1610–1615.
11. Class CA, Lukan CJ, Bristow CA, et al. Easy NanoString nCounter data analysis with the NanoTube. *Bioinformatics*. 2023;39:btac762.
12. Diaz-Siso JR, Bueno EM, Sisk GC, et al. Vascularized composite tissue allotransplantation—state of the art. *Clin Transplant*. 2013;27:330–337.
13. Cipriani R, Contedini F, Santoli M, et al. Abdominal wall transplantation with microsurgical technique. *Am J Transplant*. 2007;7:1304–1307.
14. Levi DM, Tzakis AG, Kato T, et al. Transplantation of the abdominal wall. *Lancet*. 2003;361:2173–2176.
15. Todeschini M, Cortinovis M, Perico N, et al. In kidney transplant patients, alemtuzumab but not basiliximab/low-dose rabbit antithymocyte globulin induces B cell depletion and regeneration, which associates with a high incidence of de novo donor-specific anti-HLA antibody development. *J Immunol*. 2013;191:2818–2828.
16. Bloom D, Chang Z, Pauly K, et al. BAFF is increased in renal transplant patients following treatment with alemtuzumab. *Am J Transplant*. 2009;9:1835–1845.
17. Heidt S, Hester J, Shankar S, et al. B cell repopulation after alemtuzumab induction—transient increase in transitional B cells and long-term dominance of Naïve B cells. *Am J Transplant*. 2012;12:1784–1792.
18. Tydén G, Genberg H, Tollemar J, et al. A randomized, doubleblind, placebo-controlled, study of single-dose rituximab as induction in renal transplantation. *Transplantation*. 2009;87:1325–1329.
19. Tomita Y, Iwadoh K, Ogawa Y, et al. Single fixed low-dose rituximab as induction therapy suppresses de novo donor-specific anti-HLA antibody production in ABO compatible living kidney transplant recipients. *PLoS One*. 2019;14:e0224203.
20. Song YH, Huh KH, Kim YS, et al. Impact of pretransplant rituximab induction on highly sensitized kidney recipients: comparison with non-rituximab group. *J Korean Surg Soc*. 2012;82:335–339.
21. Cheungpasitporn W, Thongprayoon C, Edmonds PJ, et al. The effectiveness and safety of rituximab as induction therapy in ABO-compatible non-sensitized renal transplantation: a systematic review and meta-analysis of randomized controlled trials. *Ren Fail*. 2015;37:1522–1526.
22. Lowsky R. Thymoglobulin and regulatory T cells in organ and hematopoietic cell transplantation. *Transplantation*. 2007;84:S20–S26.
23. Schmitz R, Fitch ZW, Schroder PM, et al. B cells in transplant tolerance and rejection: friends or foes? *Transplant Int*. 2020;33:30–40.
24. DiLillo DJ, Griffiths R, Seshan SV, et al. B lymphocytes differentially influence acute and chronic allograft rejection in mice. *J Immunol*. 2011;186:2643–2654.
25. Bouaziz JD, Yanaba K, Venturi GM, et al. Therapeutic B cell depletion impairs adaptive and autoreactive CD4+ T cell activation in mice. *Proc Natl Acad Sci U S A*. 2007;104:20878–20883.
26. Caporaso JG, Lauber CL, Costello EK, et al. Moving pictures of the human microbiome. *Genome Biol*. 2011;12:R50.
27. Edmonds-Wilson SL, Nurinova NI, Zapka CA, et al. Review of human hand microbiome research. *J Dermatol Sci*. 2015;80:3–12.
28. Hoisington AJ, Stamper CE, Bates KL, et al. Human microbiome transfer in the built environment differs based on occupants, objects, and buildings. *Sci Rep*. 2023;13:6446.
29. Milek D, Reed LT, Echternacht SR, et al. A systematic review of the reported complications related to facial and upper extremity vascularized composite allotransplantation. *J Surg Res*. 2023;281:164–175.
30. Rifkin WJ, David JA, Plana NM, et al. Achievements and challenges in facial transplantation. *Ann Surg*. 2018;268:260–270.
31. Ramly EP, Alfonso AR, Berman ZP, et al. The first successful combined full face and bilateral hand transplant. *Plast Reconstr Surg*. 2022;150:414–428.
32. Gelb BE, Diaz-Siso JR, Plana NM, et al. Absence of rejection in a facial allograft recipient with a positive flow crossmatch 24 months after induction with rabbit anti-thymocyte globulin and anti-CD20 monoclonal antibody. *Case Rep Transplant*. 2018;2018:7691072.
33. Barth RN, Rodriguez ED, Mundinger GS, et al. Vascularized bone marrow-based immunosuppression inhibits rejection of vascularized composite allografts in nonhuman primates. *Am J Transplant*. 2011;11:1407–1416.
34. Lin CH, Anggelia MR, Cheng HY, et al. The intragraft vascularized bone marrow component plays a critical role in tolerance induction after reconstructive transplantation. *Cell Mol Immunol*. 2021;18:363–373.
35. Kumagai S, Togashi Y, Kamada T, et al. The PD-1 expression balance between effector and regulatory T cells predicts the clinical efficacy of PD-1 blockade therapies. *Nat Immunol*. 2020;21:1346–1358.
36. Grosso JF, Kelleher CC, Harris TJ, et al. LAG-3 regulates CD8+ T cell accumulation and effector function in murine self- and tumor-tolerance systems. *J Clin Invest*. 2007;117:3383–3392.
37. Angin M, Brignone C, Triebel F. A LAG-3–specific agonist antibody for the treatment of T cell–induced autoimmune diseases. *J Immunol*. 2020;204:810–818.
38. Ellis J, Marks DJB, Srinivasan N, et al. Depletion of LAG-3+ T cells translated to pharmacology and improvement in psoriasis disease activity: a phase I randomized study of mAb GSK2831781. *Clin Pharmacol Ther*. 2021;109:1293–1303.
39. Lino AC, Dang VD, Lampropoulou V, et al. LAG-3 inhibitory receptor expression identifies immunosuppressive natural regulatory plasma cells. *Immunity*. 2018;49:120–133.e9.
40. Marques RE, Guabiraba R, Russo RC, et al. Targeting CCL5 in inflammation. *Expert Opin Ther Targets*. 2013;17:1439–1460.
41. Friedman O, Carmel N, Sela M, et al. Immunological and inflammatory mapping of vascularized composite allograft rejection processes in a rat model. *PLoS One*. 2017;12:e0181507.
42. Choy JC. Granzymes and perforin in solid organ transplant rejection. *Cell Death Differ*. 2010;17:567–576.

43. Suárez-Álvarez B, López-Vázquez A, Baltar JM, et al. Potential role of NKG2D and its ligands in organ transplantation: new target for immunointervention. *Am J Transplant*. 2009;9:251–257.
44. Zou Y, Stastny P. Role of MICA in the immune response to transplants. *Tissue Antigens*. 2010;76:171–176.
45. Ito A, Shimura H, Nitahara A, et al. NK cells contribute to the skin graft rejection promoted by CD4+ T cells activated through the indirect allorecognition pathway. *Int Immunol*. 2008;20:1343–1349.
46. Halloran PF, Venner JM, Madill-Thomsen KS, et al. Review: the transcripts associated with organ allograft rejection. *Am J Transplant*. 2018;18:785–795.
47. Borges TJ, O'Malley JT, Wo L, et al. Codominant role of interferon-γ– and interleukin-17–producing T cells during rejection in full facial transplant recipients. *Am J Transplant*. 2016;16:2158–2171.
48. Rabbani PS, Rifkin WJ, Kadle RL, et al. Noninvasive monitoring of allograft rejection using a novel epidermal sampling technique. *Plast Reconstr Surg Glob Open*. 2019;7:e2368.
49. Unadkat JV, Schneeberger S, Horibe EH, et al. Composite tissue vasculopathy and degeneration following multiple episodes of acute rejection in reconstructive transplantation. *Am J Transplant*. 2010;10:251–261.